

DRAFT

Testing the Reality of Strong Magnetic Fields on T Tauri Stars: The Naked T Tauri Star Hubble 4

Christopher M. Johns-Krull^{1,2}

*Department of Physics & Astronomy, Rice University, 6100 Main St. MS-108, Houston,
TX 77005*

cmj@rice.edu

Jeff A. Valenti¹

Space Telescope Science Institute, 3700 San Martin Dr., Baltimore, MD 21210

valenti@stsci.edu

Steven H. Saar¹

Center for Astrophysics, Harvard University, 60 Cambridge Street, Cambridge, MA 02138

saar@head.cfa.harvard.edu

ABSTRACT

High resolution optical and infrared (IR) echelle spectra of the naked (diskless) T Tauri star Hubble 4 are presented. The K band IR spectra include 4 Zeeman sensitive Ti I lines along with several magnetically insensitive CO lines. Detailed spectrum synthesis combined with modern atmospheric models is used to fit the optical spectra of Hubble 4 in order to determine its key stellar parameters: $T_{\text{eff}} = 4158 \pm 56$ K; $\log g = 3.61 \pm 0.50$; $[M/H] = -0.08 \pm 0.05$; $v \sin i = 14.6 \pm 1.7$ km s⁻¹. These stellar parameters are used to synthesize K band spectra to compare with the observations. The magnetically sensitive Ti I lines are all significantly broadened relative to the lines produced in the non-magnetic model, while the magnetically insensitive CO lines are well matched by the basic non-magnetic model. Models with magnetic fields are synthesized and fit to the Ti I

¹Visiting Astronomer, Infrared Telescope Facility, operated for NASA by the University of Hawaii

²Visiting Astronomer, McDonald Observatory, operated by The University of Texas at Austin

lines. The best fit models indicate a distribution of magnetic field strengths on the stellar surface characterized by a mean magnetic field strength of 2.51 ± 0.18 kG. The mean field is a factor of 2.0 greater than the maximum field strength predicted by pressure equipartition arguments. To confirm the reality of such strong fields, we attempt to refit the observed profiles using a two component magnetic model in which the field strength is confined to the equipartition value representing plage-like regions in one component, and the field is allowed to vary in a cooler component representing spots. It is shown that such a model is inconsistent with the optical spectrum of the TiO bandhead at 7055 Å.

Subject headings: infrared: stars — stars: magnetic fields — stars: pre-main sequence — stars: individual (Hubble 4)

1. Introduction

Classical T Tauri stars (CTTSs) appear to be roughly solar mass pre-main sequence stars still surrounded by disks of material which actively accrete onto the central star. Their properties have been recently reviewed by Ménard and Bertout (1999). It is within the disks surrounding CTTSs that solar systems form. Understanding the processes through which young stars interact with and eventually disperse their disks is critical for understanding the formation of planets and the rotational evolution of stars.

Over the past several years, strong stellar magnetic fields have come to play a central role in current theories describing the interaction of a CTTS with its circumstellar accretion disks. Current theories posit that the stellar magnetic field truncates the disk at or inside the corotation radius, directing the flow of accreting disk material toward the polar regions of the central star (e.g. Camenzind 1990, Königl 1991, Cameron & Campbell 1993, Shu et al. 1994, Paatz & Camenzind 1996). This magnetospheric accretion model is driven by the need to explain how CTTSs can accrete substantial amounts of material (and presumably angular momentum), yet remain relatively slow rotators (Hartmann & Stauffer 1989). Early observations showed that CTTSs later than K7 had rotation periods of 7 - 10 days while diskless T Tauri stars (the naked TTs: NTTs) rotated with a wide range of periods (Edwards et al. 1993). While this dichotomy in the rotation rates between CTTSs and NTTs has recently been called into question (Stassun et al. 1999) for stars in the Orion Nebula Cluster, it is likely that some process must be regulating the rotation of CTTSs since many of these stars do not appear to be spun up by disk accretion. The magnetospheric accretion model provides a means of regulating the stellar rotation, and it has been used to successfully describe some of the observed characteristics of high spectral resolution line profiles observed

in CTTs (Hartmann, Hewett, & Calvet 1994; Muzerolle, Calvet, & Hartmann 1998).

The most successful approach for measuring fields on late-type stars in general has been to measure Zeeman broadening of spectral lines in unpolarized light (e.g., Robinson 1980; Saar 1988; Valenti, Marcy, & Basri 1995; Johns-Krull & Valenti 1996). For any given Zeeman σ component, the splitting resulting from the magnetic field is

$$\Delta\lambda = \frac{e}{4\pi m_e c^2} \lambda^2 g B = 4.67 \times 10^{-7} \lambda^2 g B \quad \text{mÅ kG}^{-1}, \quad (1)$$

where g is the Landé- g factor of the transition, B is the strength of the magnetic field (given in kG), and λ is the wavelength of the transition (specified in angstroms). The first direct detection of a magnetic field on a TTS was reported by Basri, Marcy, and Valenti (1992). These authors used the fact that marginally saturated magnetically sensitive lines will have an increase in their equivalent width in the presence of a magnetic field as the line components split to either side, increasing line opacity in the wings. Using this equivalent width technique, Basri et al. (1992) measured the field of the NTTS Tap 35, obtaining a value of the magnetic field strength, B , times the filling factor, f , of field regions of $Bf = 1.0 \pm 0.5$ kG. As the importance of magnetic fields on TTSs has become recognized, more effort has recently been put into their measurement. Guenther et al. (1999) used the same basic technique as Basri et al. (1992) to analyze spectra from 5 TTSs, claiming significant field detections on 2 stars.

From the perspective of cool star research, the high apparent field strengths on TTSs is a little surprising. Spruit & Zweibel (1979) computed flux tube equilibrium models, showing that magnetic field strength is expected to scale with gas pressure in the surrounding non-magnetic photosphere. Field strengths set by pressure equipartition appears to be observed in G and K dwarfs (e.g. Saar 1990, 1994, 1996) and possibly in M dwarfs (e.g. Johns-Krull & Valenti 1996). TTSs have relatively low surface gravities and hence low photospheric gas pressures, so that equipartition flux tubes would have relatively low magnetic field strengths compared to cool dwarfs. Indeed, Safer (1999) examined in some detail the ability of TTS photospheres to confine magnetic flux tubes via pressure balance with the surrounding quiet photosphere, concluding that the maximum field strength allowable on TTSs is substantially below the current detections. Safer does point out a number of potential problems in the data analysis which might affect the results of Basri et al. (1992) and Guenther et al. (1999) and lead to an overestimate of Bf on these stars. On the other hand, it is doubtful that pressure equipartition arguments should hold when the magnetic field filling factor approaches unity on the stellar surface. Saar (1996) finds that the magnetic field strength does rise above the pressure equipartition value for very active K and M dwarfs once the filling factor reaches a value near one. As a result, super-equipartition fields on TTSs, if confirmed, would be an extension of the behavior of very active main sequence stars.

Johns–Krull, Valenti, and Koresko (1999b - hereafter Paper I) have examined three (Königl 1991, Cameron & Campbell 1993, Shu et al. 1994) of the magnetospheric accretion flow theories which provide detailed analytic expressions for the surface magnetic field strength on CTTSs. In the context of these theories, the surface field strength depends on the stellar mass, radius, rotation rate, and the mass accretion rate onto the star from the disk. Taking values of these quantities from the literature, Paper I shows that the predicted magnetic field strengths vary over a large range of values, including strengths as high as 11 kG. The mass accretion rate estimates used in Paper I are preferentially those of Hartigan, Edwards, and Ghandour (1995). Gullbring et al. (1998) argue that these accretion rates are an order of magnitude too high. Paper I showed that the predicted field strengths depend on the square root of the accretion rate. Adopting the lower accretion rates favored by Gullbring et al. (1998) suggests that the fields on CTTSs should range up to ~ 4 kG, still quite a measurable value.

Paper I made use of the wavelength dependence of the Zeeman effect (see Eq. [1]) to detect actual Zeeman broadening of a Ti I line at $2.2 \mu\text{m}$ on the CTTS BP Tau, measuring an average field strength of $\bar{B} = 2.6 \pm 0.3$ kG. The detection of Zeeman broadening yields magnetic field strengths largely immune to the uncertainties pointed out by Safier (1999) in equivalent width analyses; however, Paper I points out that the observations could be reproduced by an accretion disk with unusual properties. Paper I further suggests that observations of additional IR lines (particularly magnetically insensitive CO lines) are needed to validate the magnetic field detection. Paper I also points out that the mean field detected on BP Tau is larger than that which can be confined by pressure balance with the quiet photosphere as discussed by Safier (1999); however, this is not a problem if the magnetic filling factor is unity in the visible photosphere (see also Solanki 1994, Saar 1996). Indeed, the filling factor is unity in the dipole field configurations favored in current theoretical models (Königl 1991, Cameron & Campbell 1993, Shu et al. 1994).

Another method for detecting magnetic fields is to look for net circular polarization in Zeeman sensitive lines. Observed along a line parallel to the magnetic field, the Zeeman σ components are circularly polarized, with the components split to either side of the nominal line wavelength having opposite helicity. If there is a net longitudinal component of the magnetic field on the stellar surface, net circular polarization results, and is usually easier to detect than Zeeman broadening of optical lines in unpolarized light. If the magnetic topology on the star is complex and small scale (as on the Sun), nearly equal amounts of both field polarities will generally be present producing negligible net polarization. Johns–Krull et al. (1999a) detect net polarization in the He I $\lambda 5876$ *emission* line on the CTTS BP Tau, indicating a net longitudinal magnetic field of $+2.46 \pm 0.12$ kG in the line formation region. This He I emission line is believed to form in the post-shock region where disk

material accretes onto the stellar surface (Hartmann, Hewett, & Calvet 1994; Edwards et al. 1994). If the accretion shock forms at or above the stellar surface, this observation provides additional evidence that super-equipartition fields do exist on at least one CTTS.

In an effort to further test the reality of strong magnetic fields on TTSS, we present here an analysis of the NTTS Hubble 4. We detect Zeeman broadening in four Ti I lines in the K band. Since NTTSS do not have close circumstellar accretion disks, there can be no confusing the Zeeman broadening signature in magnetically sensitive IR lines with kinematic broadening due to formation in a disk. To further verify the magnetic nature of the detected broadening, several magnetically insensitive CO lines are also observed in the IR which show no broadening beyond that expected from stellar rotation.

Hubble 4 is a K7 NTTS which shows strong, circularly polarized radio continuum emission which suggests the presence of large scale, ordered magnetic fields in this star (Skinner 1993). In the recent compilation of Briceño et al. (2002), they adopt $T_{\text{eff}} = 4060$ K and $L_{\text{bol}} = 2.7L_{\odot}$ for Hubble 4, implying $R_* = 3.4R_{\odot}$. Using the pre-main sequence evolutionary tracks of Palla and Stahler (1999), these values of the effective temperature and luminosity imply $M_* = 0.8M_{\odot}$. Combining this mass with the above radius gives an expected gravity of $\log g = 3.28$.

We present below optical and IR high resolution spectroscopy that implies strong magnetic fields are indeed present on the surface of the NTTS Hubble 4. The observations and data reduction are described in § 2. In § 3 the analysis of the data is presented: § 3.1 examines the optical data used to determine the basic atmospheric parameters of Hubble 4; while § 3.2 presents the analysis of the IR data to measure the magnetic properties of this star. A discussion of the results is given in § 4.

2. Observations and Data Reduction

We obtained optical spectra with the Sandiford cross-dispersed, echelle spectrometer (McCarthy et al. 1993) mounted at the Cassegrain focus of the 2.1 m Otto Struve telescope at the McDonald Observatory. A Reticon 1200×400 CCD was used to record each spectrum covering the wavelength interval $5803 - 7376$ Å. The spectrograph slit was approximately 1.07 arcsec wide on the sky, which projected to about 2.14 pixels on the detector, resulting in a spectral resolving power of $R \equiv \lambda/\delta\lambda = 56,000$. These spectra were reduced using an automated echelle reduction package written in IDL that is described by Hinkle et al. (2000). Data reduction included bias subtraction, flat-fielding by a normalized flat spectrum, scattered light subtraction, and optimal extraction of the spectrum. Wavelengths were deter-

mined by fitting a two-dimensional polynomial to $n\lambda$ as function of pixel and order number, n , for several hundred thorium lines observed in an internal (part of the spectrograph assembly – post telescope) lamp. In addition to observations of Hubble 4, spectra were also obtained of a rapidly rotating hot star at similar airmass to correct for contamination by telluric absorption lines. Table 1 summarizes the optical observations.

The K-band spectra presented here were obtained at the NASA Infrared Telescope Facility (IRTF) in December 1997. Observations were made with the CSHELL spectrometer (Tokunaga et al. 1990, Greene et al. 1993) using a $0''.5$ slit to achieve a spectral resolving power of $R \equiv \lambda/\Delta\lambda \sim 37,300$, corresponding to a FWHM of ~ 2.7 pixels at the 256×256 InSb array detector. A continuously variable filter (CVF) isolated individual orders of the echelle grating, and a $0.0057 \mu\text{m}$ portion of the spectrum was recorded in each of 3 settings. The first two settings (2.2218 and $2.2291 \mu\text{m}$) each contain 2 magnetically sensitive Ti I lines. The third setting ($2.3125 \mu\text{m}$) contains 9 strong, magnetically insensitive CO lines. Each star was observed at two positions along the slit separated by $10''$. The K band spectra were reduced using custom IDL software described in Paper I. The reduction includes removal of the detector bias, dark current, and night sky emission. Flat-fielding, cosmic ray removal, and optimal extraction of the stellar spectrum are also included. Wavelength calibration for each setting is based on a 3rd order polynomial fitted to $n\lambda$ for several lamp emission lines observed by changing the CVF while keeping the grating position fixed. Dividing by the order number for each setting yields the actual wavelength scale for the setting in question. In each wavelength setting, we observed Hubble 4 and a rapidly rotating star to serve as a telluric standard. In addition, observations were obtained in the two Ti I settings of the K7 dwarf 61 Cyg B. This inactive star serves as a good null field reference against which we can check details of the atomic line analysis. The IR observations are also summarized in Table 1.

3. Analysis

The wavelength dependence of the Zeeman effect makes the Ti I lines in the K band excellent probes of magnetic fields in cool stars (e.g. Saar & Linsky 1985). The goal is to measure the magnetic field on Hubble 4 by modeling the profiles of the K band absorption lines. Since other line broadening mechanisms are also potentially important, it is necessary to first demonstrate that the appearance of the spectrum in the absence of a magnetic field can be accurately predicted. Several steps are required to achieve this goal, and the work here builds on the results of Paper I. First, the optical spectrum of Hubble 4 is fit assuming no Zeeman broadening since the magnetic broadening is weak compared to rotational and

turbulent broadening at these wavelengths. This was shown to be true for BP Tau in Paper I, and the $v \sin i$ of Hubble 4 is larger than that of BP Tau, making this even more true for Hubble 4 (assuming a similar average field Bf). The regions of the optical spectrum used to fit atmospheric parameters have precise atomic line data based on fits to the solar spectrum (Paper I). In addition, these regions have been further refined in Paper I by fitting the optical spectrum of 61 Cyg B, a main sequence star with the same spectral class (K7) as Hubble 4. We reject from the analysis of TTSs some spectral features that are poorly fit in the solar spectrum, presumably due to inaccurate atomic parameters for lines that are weak or absent in the solar spectrum. Fitting the optical spectrum of Hubble 4 yields the stellar parameters T_{eff} , $\log g$, $[M/H]$, and $v \sin i$. There are various estimates of these quantities in the literature (see §1), but to guarantee self-consistency, these nonmagnetic quantities are redetermined with the same radiative transfer code and model atmosphere used in the magnetic analysis. Using the Hubble 4 model, the nonmagnetic infrared spectrum is predicted, and obvious excess broadening in the observed Ti I line profiles is noted while no such excess broadening is seen in the magnetically insensitive CO lines. This excess width in the Ti I lines is then modeled as Zeeman broadening, using a polarized radiative transfer code. Matching the observed profile then gives the strength and filling factor of magnetic regions on the surface of the star.

3.1. Fit to the Optical Spectrum

The details of the spectrum synthesis and fitting procedure are given in Paper I. Briefly, spectra for the optical wavelength regions are calculated on a grid (in T_{eff} , $\log g$, and $[M/H]$) of model atmospheres. We solve for the stellar parameters (T_{eff} , $\log g$, $[M/H]$, and $v \sin i$) using the nonlinear least squares technique of Marquardt (see Bevington & Robinson 1992). Spectra between model grid points are computed using three-dimensional linear (with respect to the model parameters T_{eff} , $\log g$, and $[M/H]$) interpolation of the resulting spectra. We interpolate the logarithm of the line depth rather than residual intensity, because the former quantity varies more slowly with changes in model parameters, yielding more accurate interpolated values. The model atmospheres are the “next generation” (NextGen) atmospheres of Allard & Hauschildt (1995). Rotational broadening in Hubble 4 is large compared to the effects of macroturbulence. This makes it difficult to solve for v_{mac} in Hubble 4, so a fixed value of 2 km s^{-1} is adopted from an extrapolation to K7 of class IV stars given in Gray (1992). In previous work (Valenti et al. 1998), it was found that microturbulence and macroturbulence were degenerate in M dwarfs, even with very high quality spectra. Therefore, for the low turbulent velocities considered here, microturbulence is neglected, allowing v_{mac} to be a proxy for all turbulent broadening in the photosphere. Spectra are synthesized in

3 optical regions, centered on 6151 Å, 6498 Å, and on the TiO bandhead at 7055 Å, which provides excellent temperature sensitivity. As described above, within these regions, only certain spectral features are used to constrain the model parameters. Following Paper I, we only use features which are modeled well in both the solar spectrum and the spectrum of 61 Cyg B, a K7V reference star.

The first line of Table 2 gives Hubble 4 model parameters determined by fitting the optical spectrum. Observed and synthetic spectra for the three wavelength intervals are shown in Figure 1. The Marquardt technique used to find the best fitting stellar parameters also gives formal uncertainties, but the actual uncertainties in derived parameters are completely dominated by systematic errors. To realistically estimate uncertainties in the derived parameters, the observations of Hubble 4 were reanalyzed with each of the 11 atomic line wavelength regions (intervals shown in Figure 1 between 6140 – 6500 Å with contiguous bold pixels) successively removed from the list of constraints. This procedure yields 11 additional values for each model parameter. The standard deviation of each derived parameter value provides an estimate of possible errors due to a bad fit in any one of the spectral segments. These uncertainty estimates are given in the second line of Table 2. The order containing the 7055 Å band head is always included in this procedure because this bandhead is such a strong temperature constraint.

The spectrum of 61 Cyg B can also be used to obtain an estimate of uncertainties in the optical analysis as was done for BP Tau in Paper I. In that paper, similar resolution spectra of 61 Cyg B covering the wavelengths used in this paper were presented and analyzed. Those data are reused here. First, the observed spectrum of 61 Cyg B is artificially broadened to $v \sin i = 14.6 \text{ km s}^{-1}$ (the value recovered for Hubble 4), using the standard rotational broadening convolution technique (Gray 1992) with limb darkening coefficients determined from the atmospheric models used to fit 61 Cyg B in Paper I. The value of v_{mac} was fixed at the value from the original fit and the remaining parameters (T_{eff} , $\log g$, $[\text{M}/\text{H}]$, and $v \sin i$) were solved for. This experiment was repeated with $v \sin i$ fixed, instead of v_{mac} . Finally, one last solution was determined letting all parameters (including $v \sin i$ and v_{mac}) float. These tests give some indication of how uncertainties in the parameters are affected by moderately rapid rotation. For each of the parameters solved for in Hubble 4, the uncertainty due to rotation is taken to be the maximum difference in these parameters between the nominal fit to 61 Cyg B and the fits obtained for the rotationally broadened spectrum. These uncertainties are given in line 3 of Table 2. The total adopted uncertainty is the sum of the uncertainties (in quadrature) produced by the scatter in the fits to the Hubble 4 data and that from the fits to the rotationally broadened 61 Cyg B spectrum. This is a rather conservative estimator, but only a few of the possible sources of systematic error have been considered. The final adopted uncertainties for Hubble 4 are reported in the fourth line of Table 2.

3.2. Fits to the Infrared Data

The IR data considered in this paper fall into two distinct categories. The first consists of the CO lines at $2.3\ \mu\text{m}$. These lines are not magnetically sensitive. In principle then, all the parameters that determine their appearance (T_{eff} , $\log g$, $[\text{M}/\text{H}]$, $v \sin i$, v_{mac}) are found from the optical fits. These lines serve as a check that the parameters determined in the optical accurately represent the IR spectrum of Hubble 4. The second category contains the magnetically sensitive Ti I lines which will allow a determination of the magnetic field on Hubble 4. Each is discussed in turn.

3.2.1. The CO Lines

Line data for CO is taken from Goorvitch (1994) for the CO $X\ \Sigma^+$ state. A model atmosphere is constructed by interpolating the grid of NextGen model atmospheres to the effective temperature, gravity, and metallicity determined above for Hubble 4 (and reported in Table 2). The CO line spectrum is computed using these parameters, and the comparison with the observed CO lines is shown in Figure 2. The agreement is excellent within the signal-to-noise of the data. In particular, the widths of the CO lines is accurately predicted by the spectrum synthesis. Again, it is important to emphasize that no free parameters (aside from a continuum normalization value) are used to match the observed and synthetic spectra. The synthesis is determined entirely by the fits to the optical spectrum of Hubble 4. Examination of Figure 2 does show that the line strengths may be off slightly, no tuning of the oscillator strengths has been attempted for the CO lines. It is their width that is of concern since these lines are insensitive to magnetic fields, and the line widths are well fit by the model.

3.2.2. The Magnetically Sensitive Ti I Lines

Ti I Oscillator Strengths

Paper I only used one Ti I line to model magnetic fields in BP Tau. BP Tau displays strong K band veiling (e.g. Johns–Krull & Valenti 2001), which made it impossible to distinguish between the effects of veiling and inaccurate oscillator strengths for the line. In the case of Hubble 4, there is no K band veiling and 4 Ti I lines are available to model. It is often the case that inadequate precision in the laboratory data or theoretical calculations results in oscillator strengths which produce synthetic lines that are a poor match to the observed

line depths. As a result, some effort was expended to check the oscillator strengths for all 4 lines as was done for the optical lines in Paper I. Matching lines in the solar spectrum is a popular method to refine oscillator strengths. Unfortunately, the 4 Ti I lines are very weak in the solar spectrum, ranging in strength from $\sim 3.50 - 10.86 \text{ m}\text{\AA}$ based on the KPNO disk center solar atlas (Livingston & Wallace 1991). The S/N of the disk center atlas becomes an issue when measuring such weak lines, particularly for the $2.2310 \mu\text{m}$ line which is the weakest of the four. Given the weakness of these Ti I lines in the solar spectrum, the Ti I gf values were checked by comparison with the spectrum of 61 Cyg B where the lines are much stronger. In addition, using 61 Cyg B to constrain the oscillator strengths serves as a good self consistency check for the synthetic spectra of Hubble 4 since both stars have the same spectral type (K7), and 61 Cyg B is modeled using the same NextGen atmospheres used to model Hubble 4. Atmospheric parameters for 61 Cyg B are taken from Paper I. Initially, the synthetic Ti I lines were weaker than the observed lines in 61 Cyg B. The gf values of the 4 Ti I lines were adjusted and synthetic models were calculated and compared to the observed profiles until χ^2 was minimized. The resulting gf values are reported in Table 3 and are used to model Hubble 4.

Single Field Component Model

The simplest model to consider with a magnetic field is one in which some fraction of the surface is covered by a field of a single strength, while the rest of the surface is field free, or *quiet*. Such a model is then specified by the field strength, B , and the filling factor, f , of the field on the surface. By analogy to the mean field direction in solar plage, we assume a radial field geometry in the photosphere for Hubble 4. On the Sun, strong magnetic field is found in both solar plage regions which are slightly hotter and brighter than the quiet atmosphere, and in sunspots which are significantly cooler than the quiet atmosphere. However, the filling factors of magnetic field reported for TTs to date (Basri et al. 1992, Guenther et al. 1999, Paper I) are very large, making it unclear that the distinction seen in the thermal structure of field regions observed on the Sun is appropriate for TTs. Additionally, magnetospheric accretion theory suggests there is strong magnetic field covering the entire surface of TTs, again making it unclear that the distinction observed on the Sun is appropriate. On the other hand, observations of photometric and line profile variability on NTTs supports the existence of brightness inhomogeneties on their surface (e.g. Herbst et al. 1987; Bouvier & Bertout 1989; Strassmeier, Welty, & Rice 1994; Joncour, Bertout, & Menard 1994) Exploring to what extent the data demand that the entire star is covered by strong field is one of the goals of the current study, and this question is investigated further below. To start with then, we model the single field component using an atmosphere that matches the overall effective temperature of the star, so that magnetic regions are neither hot like plage nor cool

like spots.

The spectrum synthesis including magnetic fields has been described in Paper I. The Marquardt technique is again used to solve for the best fitting values of the field strength and filling factor. The temperature, gravity, metallicity, rotational and turbulent broadening parameters are held fixed at the values determined in the analysis of the optical spectrum. The best fit to the IR data with a single field component model yields $B = 2.98$ kG and $f = 0.71$. In Figure 3, this model is compared to the observed spectrum and a model with no magnetic field, and the fit parameters are also given in Table 4. Clearly, the model with a magnetic field is a much better fit to the observed spectrum, yielding a reduced χ^2 of $\chi_r^2 = 1.95$ (computed considering only the points in the Ti I lines shown in bold in Figure 3). The non-magnetic model (which has no free parameters - everything is determined from the optical fits) gives $\chi_r^2 = 12.68$.

Multi-Component Field Models

While this two component model provides a fairly good fit to the observed lines, the computed 2.22112, 2.22328, and especially the 2.23106 μm lines are all weaker than the observed profiles. In Paper I, it was found that the best fit to the observed BP Tau Ti I profile was achieved with a model consisting of a handful of separate magnetic components, each with a different filling factor. This was motivated by the smooth, broad shape of the observed line profile which did not show resolved Zeeman σ components. In the case of Hubble 4 here, the higher $v \sin i$ of this star compared to BP Tau results in generally smooth profiles even when only a single magnetic component is considered (Figure 3). However, one of the hallmarks of magnetic fields is that they increase the equivalent width of partially saturated spectral lines which are Zeeman sensitive (Leroy 1962, Basri et al. 1992), and this is true of the models shown in Figure 3. The exact increase in the line equivalent width is a function of the line strength and the number and magnetic sensitivity of Zeeman components which split in response to the magnetic field (Basri et al. 1992, Guenther et al. 1999). This effect can be enhanced even further if multiple magnetic components are considered. Finally, if the fields on TTSs are dipolar in nature as assumed by theory, a distribution of field strengths is *predicted* with the maximum field strength twice that of the minimum field value. While observations do not support a dipolar geometry for the fields (e.g. Johns-Krull et al. 1999b), it is still interesting to consider multi-component magnetic field models for Hubble 4.

In the context of such models, it was found in Paper I that multicomponent models with too many field components are degenerate since the combined effects of the spectrometer resolution and stellar rotation make it difficult to constrain separate field components if their field strengths are too similar. This effective magnetic resolution was found to be ~ 2 kG

in the case of BP Tau. The larger $v \sin i$ of Hubble 4 acts to lower the effective magnetic resolution achievable on this star. An estimate can be calculated by adding in quadrature the broadening width, $\Delta\lambda$, due to the spectrometer resolution ($R = 37,300$) to the broadening produced by rotation ($\Delta\lambda = v \sin i * \lambda / c$). The resulting characteristic line width is $\Delta\lambda = 1.24 \text{ \AA}$ at the wavelength of the K band Ti I lines. Putting this into equation (1) and assuming a typical Landé- g value of 2.0 for the Ti lines gives a magnetic field strength of 2.68 kG. This should be roughly the magnetic resolution achievable with the observations analyzed here; however, simultaneous modeling of all 4 available Ti I lines (with Landé- g extending up to 2.50) mediates this effect somewhat. As a result, our analysis of Hubble 4 below has approximately the same effective magnetic resolution (2 kG) as our previous analysis of BP Tau (Paper I).

The multi-component field models are constructed by calculating synthetic spectra at specific field strengths, assigning a filling factor to each field component subject to the constraint that the total filling factor is 1.0, and then summing up the individual spectra weighted by their filling factors. To fit the observations the Marquardt technique is again used to find the optimal combination of filling factors which produces the best fit to the observed line profiles. Since there is potential degeneracy in the combination of filling factors, a Monté Carlo technique is used to test how sensitive the solution is to the assumed starting value for each filling factor. For each combination of filling factors that are being solved for, the fit is performed 100 times with randomly chosen starting values for the filling factors. The mean and standard deviation of each solved filling factor is then computed from these 100 different trials.

A total of 4 different multi-component models are considered. The model results are summarized in Table 4. Model M1 solves for the filling factors of component fields of 0 – 7 kG in 1 kG steps for a total of 8 different components. The filling factors and their standard deviations (for all models) are reported in Table 4. Also reported in the Table is the value of χ_r^2 produced by the distribution of mean filling factors. In all 4 models, this value of χ_r^2 is within 0.02 of the mean value of χ_r^2 derived from the Monté Carlo trials for a given model. Lastly, the sum of the field strength multiplied by its filling factor (ΣBf) is also given. This value corresponds to the mean field strength, \bar{B} , on the stellar surface.

Examination of model M1 shows substantial filling factors are found every 2 kG, with very little filling factor at the field values in between. It is unlikely that the true distribution on the star is so punctuated. This behavior is most likely a manifestation of the limited magnetic field resolution discussed above. Due to this limited magnetic resolution and the behavior shown in model M1, model M2 was limited to only considering field values from 0 – 6 kG in 2 kG steps. The results for model M2 are given in the third column of Table 4.

An interesting question to consider is the extent to which a quiet ($B = 0$) field component is required by the Ti I data. As mentioned above, current theories of magnetospheric accretion suggest the entire surface of TTSs is covered by kilogauss level magnetic fields. Model M1 is indeed found to have only 1% coverage on the stellar surface of field free regions. Therefore, model M3 was constructed only considering fields in the 1 – 7 kG range, again in 2 kG steps. The distribution of filling factors is reported in the fourth column of Table 4. While somewhat marginal, the reduced χ^2 of model M3 is indeed lower than that for models M1 and M2. Finally, examination of the results for models M1, M2, and M3 reveals relatively little filling factor in regions with field strengths above 5 kG. Model M4 was therefore constructed to only consider fields in the range 1 – 5 kG in 2 kG steps, and the results are reported in the final column of Table 4. This model produced the lowest value for χ_r^2 and is shown in Figure 4.

The Monté Carlo trials for the multi-component models produce fits with nearly identical values of χ_r^2 for a given model. This indicates that the χ_r^2 surface is relatively smooth, and the results are essentially insensitive to the initial guess for each model. We also note that the trial giving the minimum value of χ_r^2 for each model gives filling factors within one sigma of the mean reported in Table 4. These Monté Carlo trials do not represent the uncertainty in the actual magnetic flux, however. The difference in derived mean fields (ΣBf) for the different models suggests that systematic uncertainties arising from the model assumptions dominate the overall uncertainty. We assign a value of 2.51 kG for the mean field, which is the value for the model with the lowest χ_r^2 . To conservatively estimate the uncertainty in this mean field, the standard deviation of the mean field resulting from all the models of Table 4 except the spot field model (see below) is computed. This gives an uncertainty estimate of 0.18 kG for the mean field of Hubble 4.

Spot Fields

As described above, due to their lower surface gravity, the gas pressure in TTS photospheres is unable to confine magnetic fields stronger than about 1 kG, depending on the exact values of T_{eff} and $\log g$ in the stellar atmosphere. In addition, Safer (1999) pointed out that methods based on line equivalent widths are very sensitive to errors in the assumed T_{eff} which might lead to errors in the estimated field strength. On the other hand, the field detected on BP Tau in Paper I and on Hubble 4 above is measured by the excess *width* of magnetically sensitive photospheric lines, and the field strength is insensitive to small errors in T_{eff} ; however, it is still possible that the strong fields are confined to starspots where the field can be larger due to the larger depth of formation of the spectrum in a spot, if the solar analogy is assumed to apply for starspots. In this case though, the lower radiative surface flux emerging from

a cool spot compared to the quiet photosphere may require a corresponding increase in the filling factor of magnetic regions to produce Zeeman broadened line wings of similar depth to those shown in Figure 3. This effect is offset by the fact that the Ti I lines in the K band are quite temperature sensitive, and will be substantially stronger in a cooler atmosphere. Thus, it is an open question whether the strong fields observed on TTSs can be confined to cool starspots, with the rest of the photosphere being field free or similar to plage.

Following the solar analogy then, it can be assumed that a TTS atmosphere contains three components: field free regions, cool spots containing strong fields, and plage-like regions containing field whose strength is set by pressure balance with the surrounding quiet photosphere. Solar plage shows up as brighter regions in strong lines such as H α and Ca II H and K; however, these regions are generally not distinct in the continuum and in weak atomic lines. Therefore, it is assumed that in the region of the K band Ti I lines studied here, plage-like regions on Hubble 4 have the same temperature structure as quiet regions of the atmosphere. The field in these regions is set by the gas pressure in the quiet atmosphere. This can be estimated using the Sun and setting $B = B_{\odot}(P/P_{\odot})^{1/2}$, where P is the total gas pressure in the atmosphere. In cool stars, $P \propto g^{2/3}$ where g is the gravity (Gray 1992). Using $\log g = 4.44$ for the Sun, $\log g = 3.61$ for Hubble 4 (from Table 2), and taking $B_{\odot} = 1.70$ kG which is the maximum field reported by Rüedi et al. (1992) for solar plage, the maximum plage field for Hubble 4 is 1.24 kG. Another estimate for this value can be made by setting the magnetic pressure equal to the gas pressure in the quiet atmosphere where the temperature is equal to T_{eff} . Doing this, the plage field on Hubble 4 is estimated to be 1.26 kG. These two estimates are quite close, and the higher one (1.26 kG) is adopted for the analysis shown below. The value is sometimes referred to as the (pressure) equipartition field strength. In the interest of exploring whether such a field strength is adequate to match the observations of Hubble 4, an initial single field component fit was made fixing the magnetic field strength at $B = 1.26$ kG, allowing only the filling factor to vary. The best fit yielded $f = 0.92$, with $\chi_r^2 = 8.02$. This fit is shown in Figure 5. Allowing field only equal to the equipartition value is not adequate to match the observations of Hubble 4.

The next step is to add a starspot component to the equipartition (plage-like) component. The spot field strength is treated as a free parameter; however, it is necessary to fix the temperature of the spots relative to the quiet photosphere to a specific value. Multi-color photometric monitoring (see Herbst et al. 1994 and references therein) and Doppler imaging analysis of TTSs (Strassmeier, Welty, & Rice 1994; Joncour, Bertout, & Menard 1994; Joncour, Bertout, & Bouvier 1994; Hatzes 1995; Rice & Strassmeier 1996; Johns-Krull & Hatzes 1997) finds a typical spot temperature ~ 1000 K cooler than the quiet regions, so this temperature difference is assumed here.

If it is assumed that all the field found above in the single field component fit is in a cool spot ($f_s = 0.59$) with a temperature 1000 K below that in the non-magnetic atmosphere, the temperature in the non-magnetic atmosphere must be larger than 4158 K (T_{eff} found above) so that the overall effective temperature is 4158 K. If T_q is the temperature in the quiet atmosphere and f_s is the filling factor of starspots, then this temperature is related to the stellar effective temperature by $(1 - f_s)T_q^4 + f_s(T_q - 1000)^4 = T_{\text{eff}}^4$ if the spot temperature is fixed 1000 K below T_q , and the filling factors are area filling factors (as they are in the synthetic modeling below). A first guess is obtained by setting $T_{\text{eff}} = 4158$ K and $f = 0.59$, which gives $T_q = 4660$ K. Guenther et al. (1999) point out that the filling factor of magnetic regions should be higher if these regions are in fact cool spots due to the lower continuum flux. This effect is minimized in the IR region where the brightness contrast between a $T_{\text{eff}} = 4660$ K and $T_{\text{eff}} = 3660$ K atmosphere is smaller than in the optical. This effect is also counteracted for the Ti I lines studied here since they grow in strength substantially as the temperature falls. Therefore, a first attempt was made assuming a spot temperature of $T_s = 3660$ K and a quiet and plage temperature of $T_q = T_p = 4660$ K. Again, the plage field strength is held fixed at 1.26 kG. The spot field strength, B_s , and filling factor, f_s , as well as the plage filling factor, f_p , are allowed to vary, and the quiet filling factor is given by $f_q = 1 - f_s - f_p$. Synthetic models were computed on a grid of NextGen atmospheres and these were interpolated in the same fashion as done for the optical spectra (see Paper I) to obtain spectra for the spot, plage, and quiet regions. The Marquardt method was used again to fit the Ti I line profiles. The spots and plage-like regions are assumed to be evenly distributed over the stellar surface. The best fit is shown in Figure 5 and has $f_q = 0.42$, $f_p = 0.00$, $f_s = 0.58$, and $B_s = 2.97$ kG. The average field on the stellar surface is then $\Sigma B f = 1.72$ kG. This fit gives $\chi_r^2 = 1.73$, equal to the fit of model M4 in Table 4. The fit parameters are also given in Table 4.

The quality of the spot fit suggests that the strengthening of the Ti I line in the cool spot atmosphere completely offsets the lower continuum brightness of the spot region relative to the quiet region. It is surprising that the best fit is obtained with only spot and quiet regions, without any plage like regions on the surface. At the relatively low field (1.26 kG) for the plage like regions, the dominant effect on the spectrum is to enhance the equivalent width of the lines somewhat. Due to the large $v \sin i$ of Hubble 4, this makes the Ti I lines slightly deeper, but not appreciably broader. However, the Ti lines grow significantly in strength in the relatively cool atmosphere of the spot regions. Therefore, there is no need to include plage like regions to obtain the best fit. Recall also, that the multi-component fits indicate our magnetic resolution is ~ 2 kG, so it appears the plage like component is simply degenerate and is consistently driven to zero filling factor by the fitting routine.

In addition to the Ti I lines visible in Figure 5, attention should be paid to the Sc I

2.2266 μm line. In the fit allowing for cool spots, this Sc I line is noticeably stronger than in the observations and is stronger than in the single field component and multi component models. Many Sc I lines in this region of the spectrum possess a significant nuclear spin which results in hyperfine splitting of the lines. We inspected a high resolution ($R = 225,000$) FTS spectrum of this line retrieved from the NSO Digital Library (<http://diglib.nso.edu>), and find that this line displays very small hyperfine structure. In addition, this line is relatively weak in Hubble 4, so hyperfine splitting has only a small effect on the equivalent width (though we note, any increase in equivalent width would occur in both the M4 and spot models, with the spot model still a poorer fit). All together, the influence of hyperfine splitting has less than about a $\sim 5\%$ effect on the line equivalent width. Such splitting is ignored here, and the line is treated as magnetic following LS coupling. The poorer fit of the spot model relative to all the non-spot models in the Sc I line suggests that the reality of such large spot regions can be tested by strongly temperature sensitive lines. The χ_r^2 values quoted above for all the magnetic models are based only on pixels encompassing the Ti I lines. If the Sc I line is also included, the spot model above gives $\chi_r^2 = 2.19$ (Sc I pixels used for χ_r^2 calculation are shown in Figure 5). On the other hand, model M4 of Table 4 and Figure 4 gives $\chi_r^2 = 1.94$ when including the Sc I line. This suggests the spot model is not the best description of the fields on Hubble 4.

A more sensitive test of the spot model just described is to look again at the optical spectrum analyzed in §3.1. The TiO bandhead at 7055 Å is a very temperature sensitive diagnostic at a spectral type of K7. The optical spectrum for the spot model shown in Figure 5 is shown in Figure 1. This model was computed without magnetic fields, and thus represents only the effect of the two temperature components. In Paper I, it was shown that strong magnetic fields such as those found above for Hubble 4 have a very small effect on the appearance on the optical spectrum in these regions for stars with large $v \sin i$ ($> 10 \text{ km s}^{-1}$) as the case here. In addition, the original fits shown in Figure 1 are also calculated ignoring the magnetic field. As quoted in §3.1, the original fits produce a reduced $\chi^2 = 5.20$, whereas the spot model fit of Figure 1 give reduced $\chi_r^2 = 12.62$. Clearly, such a spot model is not a better fit to the overall spectrum.

4. Discussion

Using high resolution optical spectra, we have determined atmospheric parameters (Table 2) for Hubble 4 which agree well with most published estimates. As described in §1, Briceño et al. (2002) adopt $T_{\text{eff}} = 4060 \text{ K}$ and $L_{\text{bol}} = 2.7L_{\odot}$ for Hubble 4, implying $R_* = 3.4R_{\odot}$. Using the pre-main sequence evolutionary tracks of Palla and Stahler (1999),

these values of the effective temperature and luminosity imply $M_* = 0.8M_\odot$. Combining this mass with the above radius gives an expected gravity of $\log g = 3.28$. The fit to the optical spectrum finds $T_{\text{eff}} = 4158 \pm 56$ K and $\log g = 3.61 \pm 0.50$ in good agreement with these numbers. The spectroscopically determined temperature can be combined with the luminosity above (assuming a 10% uncertainty) to find $R_* = 3.19 \pm 0.33$. This in turn can be used with our spectroscopic estimate of gravity to obtain $M_* = 1.5M_\odot$ with a factor of 1.8 uncertainty, driven almost entirely by the uncertainty in the fitted gravity. While not a precise measure of the stellar mass, it is interesting to note that the mass determined here is larger than that estimated from evolutionary tracks. The same result was found for BP Tau in Paper I, albeit with similarly large uncertainty. In their study of stars with dynamical mass determinations, Hillenbrand and White (2004) also find that evolutionary tracks tend to underpredict the mass in lower mass stars.

In Paper I, clear excess broadening of the $2.2233 \mu\text{m}$ Ti I line was interpreted as Zeeman broadening due to the presence of a mean magnetic field of 2.6 kG in the photosphere of BP Tau. However, that paper pointed out that a disk with unusual properties could in principle produce the same kind line broadening as observed. Here, the NTTS Hubble 4 is studied which lacks a close circumstellar disk. Therefore, the near IR Ti I lines from this star must be photospheric in origin. As for BP Tau in Paper I, clear excess broadening is seen in the 4 observed magnetically sensitive $2.2 \mu\text{m}$ Ti I lines relative to what is expected from a model calculation based on fitting lines observed in the optical at high spectral resolution. Each of the four Ti lines has a different Zeeman splitting pattern and hence a different predicted response to magnetic fields. The observed line widths and strengths respond as predicted for Zeeman broadening, adding support for this interpretation. The fit based on the optical spectrum accurately reproduces magnetically insensitive $2.3 \mu\text{m}$ CO lines. The widths of infrared CO lines and all optical lines are dominated by rotational broadening. The infrared atomic lines show significant additional broadening that must be due to a process that preferentially affects the IR lines. Zeeman broadening is such a process. Therefore, Zeeman broadening due to strong stellar magnetic fields appears to be the only explanation for the large linewidths of the Ti I lines.

Modeling the observed Ti lines with magnetic fields produces good fits to the observed spectra. Unlike BP Tau in Paper I, the evidence demanding the presence of multiple magnetic components with different field strengths on the surface of Hubble 4 is not as strong, though it is present. This appears to be the result of the larger $v \sin i$ of Hubble 4 (14.6 km s^{-1}) compared to that of BP Tau (10.2 km s^{-1}), which yields somewhat poorer Zeeman resolution in our analysis of Hubble 4. The best fitting single field component field model gives $\chi_r^2 = 1.95$, while the best fitting multi-component model (M4 of Table 4) gives $\chi_r^2 = 1.73$. It is interesting to note that the best fit multi-component model does not have a field free

component. Thus, with the current data it is not possible to show that Hubble 4 possesses any field free regions.

The mean magnetic field on the surface is computed from the models by summing the quantity Bf over the different components used in the model. This mean field we find for Hubble 4 is 2.51 ± 0.18 kG. This field strength is comparable to the field strength required for some current magnetospheric accretion models (Paper I). Equipartition arguments suggest that the maximum magnetic field strength allowable on the surface of a TTS may be determined by pressure equilibrium with the surrounding non-magnetic (quiet) photosphere. For Hubble 4, the equipartition field strength is found to be ~ 1.26 kG in §3.2.2. Thus, the mean field of 2.51 kG found for this star is a factor of ~ 2.0 times too strong to be in pressure equipartition. Model M4 has a 12% filling factor for 5 kG fields, which are a factor of ~ 4 too strong to be confined by the gas pressure of the quiet photosphere. However, pressure equilibrium arguments (e.g. Spruit & Zweibel 1979, Saar 1996, Safer 1999) only apply if there are quiet regions on the star, and as discussed above, the data are actually fit better if there are no such regions on the star. Paper I found that equipartition was violated on BP Tau and Saar (1996) found that it is violated on a few very active K and M dwarfs. While pressure equipartition has been suggested as a mechanism for determining the photospheric magnetic field strength on cool stars (see also Rajaguru, Kurucz, & Hasan 2002), it does not appear to hold for very active stars. Indeed, it is expected that B can exceed pressure equipartition when $f \approx 1$ (Solanki 1994). In addition, the magnitude of velocity flows external to the magnetic flux tubes may be important in determining both the distribution function (Bunte & Saar 1993) and magnitude (Solanki 1996) of magnetic field strengths in cool stars. The solar chromosphere and corona also violate equipartition, with the magnetic field dominating the gas pressure in these regions. Perhaps it should not be surprising that very active stars extend this region of magnetic field dominance to deeper layers of the atmosphere.

The strong magnetic fields inferred on the surface of Hubble 4 dominate the gas pressure throughout the depth of the photospheric model. It is reasonable to ask if this magnetic dominance continues to deep layers of the star, possibly altering its structure. To investigate this, a polytropic stellar structure model was calculated appropriate for fully convective stars (polytropic index 1.5, e.g. Clayton 1983). As the calculation moves into the star, a decision must be made regarding how to scale the magnetic field to account for the smaller surface area it fills at smaller radii. Straight flux conservation would imply scaling with R^2 ; however, there are no magnetic monopoles. Dipolar scaling could be used instead. In either case, it turns out not to matter significantly which is chosen as the gas pressure quickly becomes stronger than the magnetic field pressure in the stellar structure calculation. This occurs about $\sim 0.5\%$ of the way into the star, or at a radius of $R \sim 0.995R_*$. So, while the

photosphere of the star may be dominated by magnetic pressure, the star as a whole is not. In the photosphere though, it is interesting to consider the appearance of star like Hubble 4 which seems to be dominated by magnetic pressure. Do the traditional solar features such as granulation, plage, and spots that are visible in the solar photosphere also appear on such a magnetic star? Spots clearly appear on these stars (e.g. Bouvier & Bertout 1989), but it is almost certain that these structures are modified by the strong fields. Pevtsov et al. (2003) find that X-ray emission from TTSs is low as a group considering their strong magnetic fields. This is confirmed by Feigelson et al. (2003) who find that TTSs in the Orion Nebular Cluster saturate their X-ray emission at a level an order of magnitude below where main sequence star do. Perhaps this is because convection is inhibited throughout the atmosphere of TTSs due to their strong magnetic fields, in the same way convection is diminished in sunspots. The weaker convection may set a limit on the mechanical energy available to heat the coronae of TTSs and produce X-rays. If this is the case, studies of line bisectors in TTSs should show a systematic difference relative to main sequence stars of the same spectral type; however, such work is difficult due to line crowding at the typically late spectral types of these stars and due to their relative faintness.

Safier (1999) originally called into question magnetic field results for TTS based on the analysis of equivalent widths (e.g. Basri et al. 1992, Guenther et al. 1999). It is certainly true that great care must be taken when using line equivalent widths to detect stellar magnetic fields; however, the analysis presented above is based on direct detection of Zeeman broadening in the spectral lines. This broadening shows that Hubble 4 has a large filling factor of very strong (~ 3 kG based on the single component model) field. On the Sun, such strong field is found only in sunspots, which form deeper in the photosphere than plage, due to lower gas density in the spot atmosphere. It is therefore interesting to consider whether the strong fields on TTS are confined to large spots, particularly since large spots are routinely found in photometric monitoring studies (e.g. Petrov et al. 1994) and in Doppler imaging studies (e.g. Johns-Krull & Hatzes 1997) of TTS. Guided by these studies, a model was constructed in which fields stronger than could be supported by pressure equilibrium were assumed to be in spots 1000 K cooler than the quiet photosphere. The continuum difference between spotted and non-spotted regions acts to increase the resulting filling factor of strong field regions (e.g. Guenther et al. 1999); however, it was found that this effect was essentially cancelled by the increase in the line strength of the K band Ti I lines formed in the cool spot atmosphere. The spot model field strength is an insignificant 8 G lower than that of the single component model, and the filling factor is actually reduced by 13%. Such a spot model is successful at reproducing the IR observations of the Ti lines; however, it predicts a very poor fit to the optical spectrum, particularly in the TiO bandhead at 7055 Å. Thus it appears that the strong fields on Hubble 4 are not confined to cool spots (or at

least, not *only* confined to cool spots), but additional work is needed to confirm this point.

Realistic models of spot atmospheres are needed to make further progress on testing whether cool spots contribute at all to the magnetic fields we have detected on TTSs. The model used above was simply that of a cooler star, with the same gravity and metallicity as that found for Hubble 4. On the Sun, magnetic pressure support partially evacuates the gas in a spot, changing its density compared to the quiet atmosphere. Such effects need to be considered for TTS (and other cool stars such as dMe stars). In addition, since it appears that the strong magnetic fields of TTS may also be present in the quiet photosphere, atmospheric models taking into account the magnetic pressure support should also be considered for this component of the atmosphere. Such a modeling effort is well beyond the scope of the current paper, but these results should be regarded as an appeal to theoreticians to begin to consider such problems, particularly since the data presented here clearly indicates the presence of strong magnetic fields on a large portion of Hubble 4. Such strong fields have also been inferred for a handful of other TTSs (Basri et al. 1992, Guenther et al. 1999, Paper I), and these strong fields are likely to be a common feature of TTSs given their strong X-ray emission (e.g. Feigelson et al. 2003).

CMJ-K would like to acknowledge partial support from the NASA Origins program through grant number NAG5-13103. SHS would like to acknowledge support from NSF grant 9528563 and a NASA Origins program grants NAG5-10360 and NNG04GL54G. We wish to thank the referee, Gibor Basri, for his thoughtful comments on the original manuscript.

REFERENCES

- Allard, F. & Hauschildt, P.H. 1995, in *Bottom of the Main Sequence and Beyond*, ed. C.G. Tinney (Berlin: Springer), 32
- Basri, G., Marcy, G. W., & Valenti, J. A. 1992, *ApJ*, 390, 622
- Bevington, P. R. & Robinson, D. K. 1992, *Data Reduction and Error Analysis for the Physical Sciences*, (New York: McGraw Hill)
- Bouvier, J. & Bertout, C. 1989, *A&A*, 211, 99
- Briceño, C., Luhman, K. L., Hartmann, L., Stauffer, J. R., & Kirkpatrick, J. D. 2002, *ApJ*, 580, 317
- Bünke, M., Saar, S. H. 1993, *A&A* 271, 167
- Camenzind, M. 1990, *Rev. Modern Astron.*, (Berlin: Springer-Verlag), 3, 234
- Cameron, A. C. & Campbell, C. G. 1993, *A&A*, 274, 309
- Clayton, D. D. 1983, *Principles of Stellar Evolution and Nucleosynthesis*, (Chicago: The University of Chicago Press)
- Edwards, S., Strom, S. E., Hartigan, P., Strom, K. M., Hillenbrand, L. A., Herbst, W., Attridge, J., Merrill, K. M., Probst, R., & Gatley, I. 1993, *AJ*, 106, 372
- Feigelson, E. D., Gaffney, J. A., Garmire, G., Hillenbrand, L. A., & Townsley, L. 2003, *ApJ*, 584, 911
- Goorvitch, D. 1994, *ApJS*, 95, 535
- Gray, D. F. 1992, *The Observation and Analysis of Stellar Photospheres*, (Cambridge: Cambridge Univ. Press)
- Greene, T. P., Tokunaga, A. T., Toomey, D. W., & Carr, J. B. 1993, *Proc. SPIE*, 1946, 313
- Guenther, E. W., Lehmann, H., Emerson, J. P., & Staude, 1999, *A&A*, 341, 768
- Gullbring, E., Hartmann, L., Briceño, C., & Calvet, N. 1998, *ApJ*, 492, 323
- Hartigan, P., Edwards, S., & Ghandour, L. 1995, *ApJ*, 452, 736
- Hartmann, L., Hewett, R., & Calvet, N. 1994, *ApJ*, 426, 669
- Hartmann, L. & Stauffer, J. R. 1989, *AJ*, 97, 873
- Hatzes, A. P. 1995, *ApJ*, 451, 784
- Herbst, W., Booth, J. F., Koret, D. L., Zajtseva, G. V., Shakhovskaya, N. I., Vrba, F. J., Covino, E., Terranegra, L., Vittone, A., Hoff, D., Kelsey, L., Lines, R., & Barksdale, W. 1987, *AJ*, 94, 137

- Herbst, W., Herbst, D. K., Grossman, E. J., & Weinstein, D. 1994, *AJ*, 108, 1906
- Hillenbrand, L. A. & White, R. J. 2004, *ApJ*, 604, 741
- Hinkle, K., Wallace, L., Valenti, J., & Harmer, D. 2000, *Visible and Near Infrared Atlas of the Arcturus Spectrum 3727-9300 Å* ed. K. Hinkle, L. Wallace, J. Valenti, & D. Harmer. (San Francisco: ASP) ISBN: 1-58381-037-4
- Johns–Krull, C. M. & Hatzes, A. P. 1997, *ApJ*, 487, 896
- Johns–Krull, C. M. & Valenti, J. A. 1996, *ApJ*, 459, L95
- Johns–Krull, C. M. & Valenti, J. A. 2001, *ApJ*, 561, 1060
- Johns–Krull, C. M., Valenti, J. A., Hatzes, A. P., & Kanaan, A. 1999a, *ApJ*, 510, L41
- Johns–Krull, C. M., Valenti, J. A., & Koresko, C. 1999b, *ApJ*, 516, 900 (Paper I)
- Joncour, I., Bertout, C., & Bouvier, J. 1994, *A&A*, 291, L19
- Joncour, I., Bertout, C., & Menard, F. 1994, *A&A*, 285, L25
- Königl, A. 1991, *ApJ*, 370, L39
- Leroy, J. L. 1962, *Ann. d’Ap.*, 25, 127
- Livingston, W. & Wallace, L. 1991, NSO Technical Report # 91-001
- McCarthy, J. K., Sandiford, B. A., Boyd, D., & Booth, J. 1993, *PASP*, 105, 881
- Ménard, F. & Bertout, C. 1999, *NATO ASIC Proc. 540: The Origin of Stars and Planetary Systems*, 341
- Muzerolle, J., Calvet, N.; & Hartmann, L. 1998, *ApJ*, 492, 743
- Paatz, G. & Camenzind, M. 1996, *A&A*, 308, 77
- Palla, F. & Stahler, S. W. 1999, *ApJ*, 525, 772
- Petrov, P. P., Shcherbakov, V. A., Berdyugina, S. V., Shevchenko, V. S., Grankin, K. N., & Melnikov, S. Y. 1994, *A&AS*, 107, 9
- Pevtsov, A. A., Fisher, G. H., Acton, L. W., Longcope, D. W., Johns–Krull, C. M., Kankelborg, C. C., & Metcalf, T. R. 2003, *ApJ*, 598, 1387
- Rajaguru, S. P., Kurucz, R. L., & Hasan, S. S. 2002, *ApJ*, 565, L101
- Rice, J. B. & Strassmeier, K. G. 1996, *A&A*, 316, 164
- Robinson, R. D. 1980, *ApJ*, 239, 961
- Rüedi, I., Solanki, S. K., Livingston, W., & Stenflo, J. O. 1992, *A&A*, 263, 323
- Saar, S. H. 1988, *ApJ*, 324, 441

- Saar, S. H. 1990, IAU Symp. 138, Solar Photosphere: Structure, Convection, and Magnetic Fields, ed. J. O. Stenflo (Dordrecht: Kluwer), 427
- Saar, S. H. 1994, IAU Symp. 154, Infrared Solar Physics, eds. D. M. Rabin et al. (Dordrecht: Kluwer), 493
- Saar, S. H. 1996, IAU Symp. 176, Stellar Surface Structure, eds. K. G. Strassmeier & J. L. Linsky (Dordrecht: Kluwer), 237
- Saar, S. H. & Linsky, J. L. 1985, ApJ, 299, L47
- Safier, P. N. 1999, ApJ, 510, 127
- Shu, F. H., Najita, J., Ostriker, E., Wilkin, F., Ruden, S., & Lizano, S. 1994, ApJ, 429, 781
- Skinner, S. L. 1993, ApJ, 408, 660
- Solanki, S.K. 1994, in Cool Stars, Stellar Systems, and the Sun, Eighth Cambridge Workshop. ASP Conference Series Vol. 64, ed. J.-P. Caillault, 477
- Solanki, S.K. 1996, IAU Symp. 176, in Stellar Surface Structure, eds. K. G. Strassmeier & J. L. (Dordrecht: Kluwer), 201
- Spruit, H. C., & Zweibel, E. G. 1979, Sol. Phys., 62, 15
- Stassun, K. G., Mathieu, R. D., Mazeh, T., & Vrba, F. J. 1999, AJ, 117, 2941
- Strassmeier, K. G., Welty, A. D., & Rice, J. B. 1994, A&A, 285, L17
- Tokunaga, A. T., Toomey, D. W., Carr, J., Hall, D. N. B., & Epps, H. W. 1990, Proc. SPIE, 1235, 131
- Valenti, J. A., Marcy, G. W., & Basri, G. 1995, ApJ, 439, 939
- Valenti, J. A., Piskunov, N., & Johns-Krull, C. M. 1998, ApJ, 498, 851

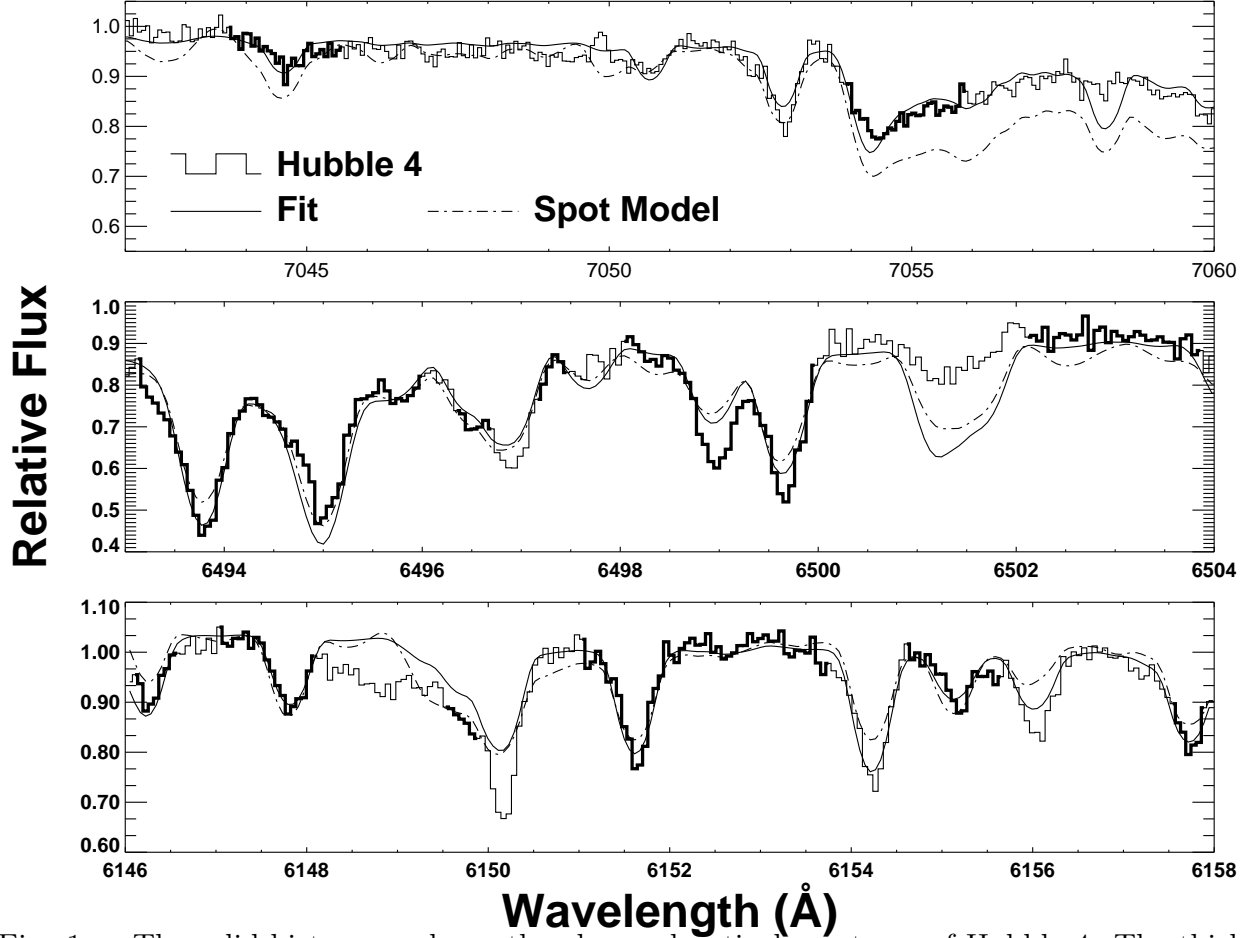


Fig. 1.— The solid histogram shows the observed optical spectrum of Hubble 4. The thick portions of the histogram show the regions of the spectrum actually used in the fit. The smooth solid curve shows the best fitting model spectrum. The dash-dot curve shows the spectrum produced by the model in which strong fields are confined to cool starspots.

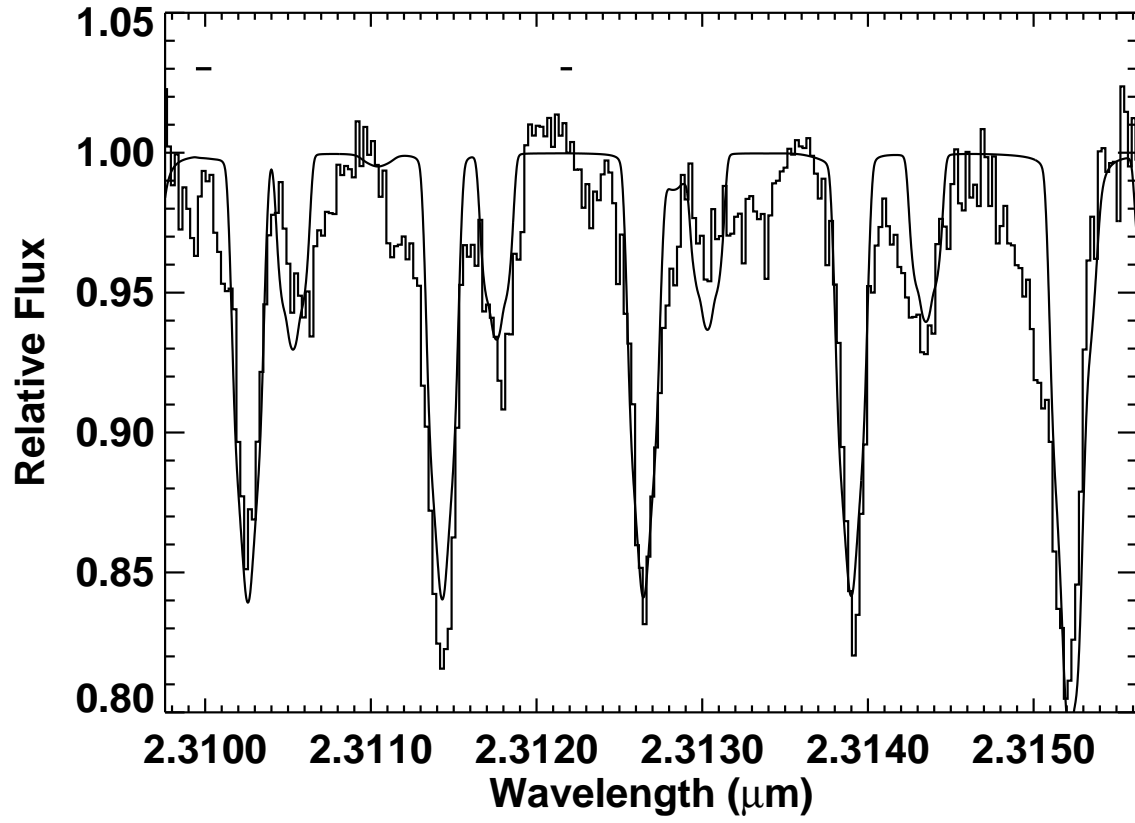


Fig. 2.— The solid histogram shows the observed CO lines of Hubble 4. The smooth solid curve shows model spectrum produced by fitting the optical spectrum. No fitting was done to the CO lines.

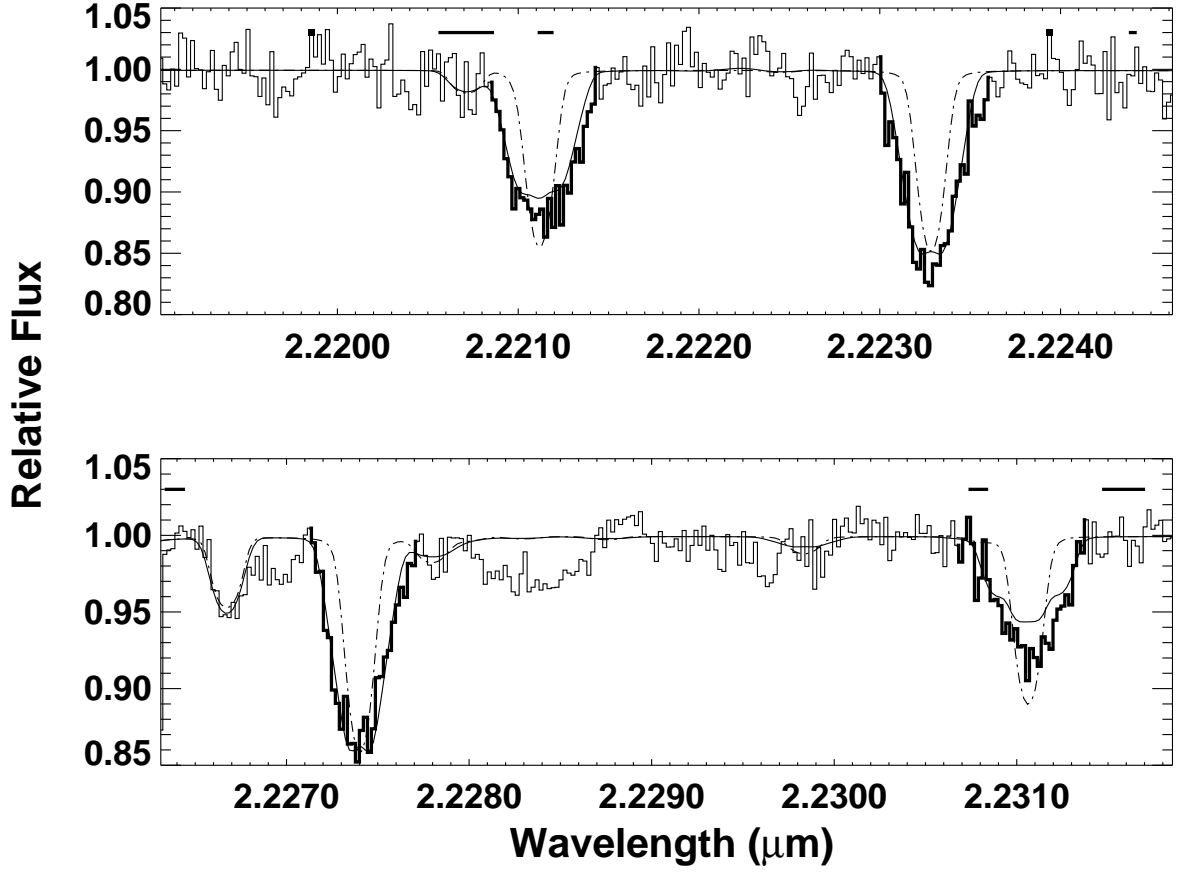


Fig. 3.— The solid histogram shows the observed Ti I lines of Hubble 4. The thick portions of the histogram show the regions of the spectrum actually used in the fit. The smooth solid curve shows the best fitting model spectrum produced with a single magnetic region with $B = 2.98$ kG and $f = 0.71$. The dash-dot curve shows the spectrum produced by a model with no magnetic fields. Horizontal bold lines at relative flux of 1.03 indicate where telluric corrections exceeded 5% of the relative flux.

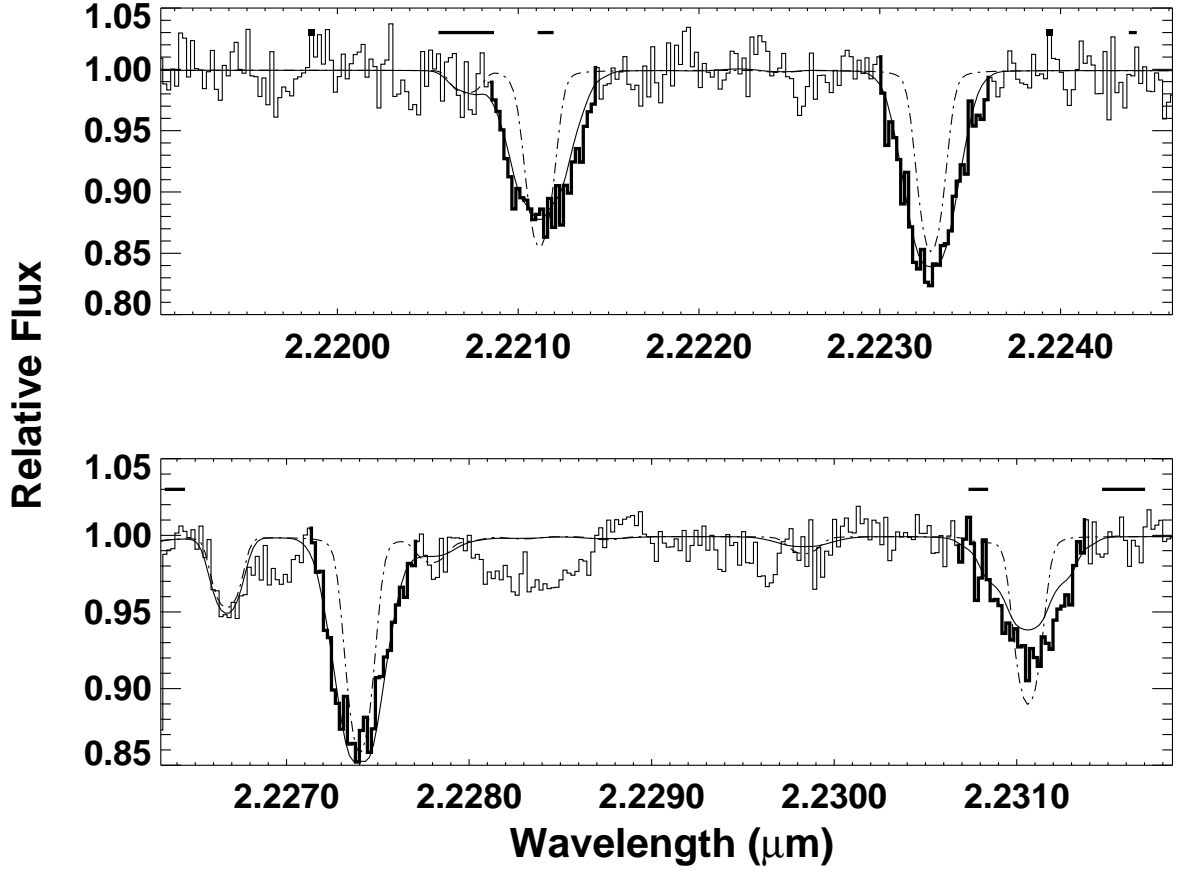


Fig. 4.— The solid histogram again shows the observed Ti I lines of Hubble 4. The thick portions of the histogram show the regions of the spectrum actually used in the fit. The smooth solid curve shows the best fitting spectrum from the multi component model M4 of Table 4. Again, the dash-dot curve shows the spectrum produced by a model with no magnetic fields. Again, horizontal bold lines at relative flux of 1.03 indicate where telluric corrections exceeded 5% of the relative flux.

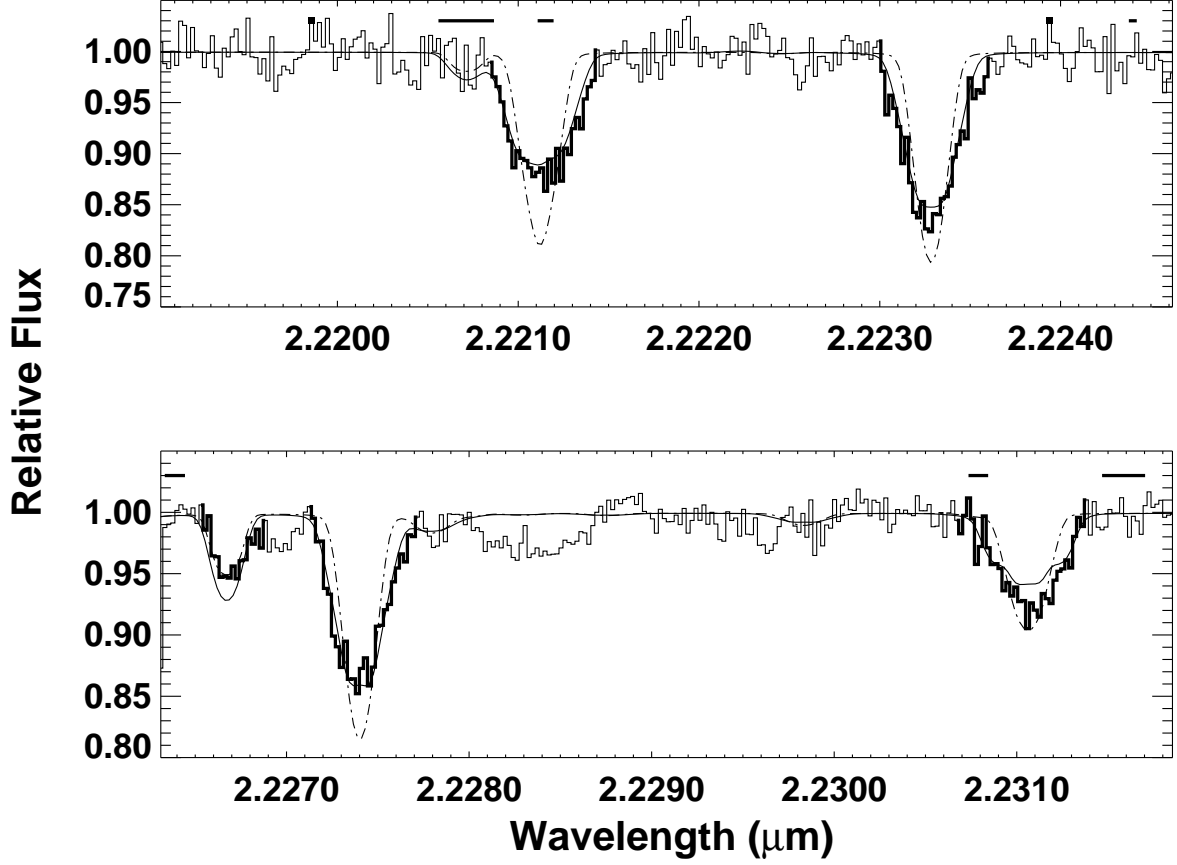


Fig. 5.— The solid histogram again shows the observed Ti I lines of Hubble 4. The thick portions of the histogram show the regions of the spectrum actually used in the fit, now including the Sc I line at $2.2266 \mu\text{m}$ which is used in the comparison of the spot model (see text). The smooth solid curve shows the best fitting spectrum produced when the strong magnetic fields are restricted to cool starspots. The dash-dot curve shows the spectrum produced the best fitting model in which the strength of the magnetic field is restricted to 1.26 kG which is the value expected when the fields are in pressure equilibrium with the surrounding quiet photosphere. Again, horizontal bold lines at relative flux of 1.03 indicate where telluric corrections exceeded 5% of the relative flux.

Table 1. Observations

Star	Date UT	Start Time UT	N_{exp}	Total Exp. Time (s)	Region	S/N
61 Cyg B	Dec. 12, 1996	5:19	6	300	2.2218 μm	180
HR 1044 ^a	Dec. 12, 1996	6:21	10	2000	2.2218 μm	120
Hubble 4	Dec. 19, 1997	9:05	12	3600	2.3125 μm	90
HR 1666 ^a	Dec. 19, 1997	11:08	4	400	2.3125 μm	250
Hubble 4	Dec. 19, 1997	13:07	10	3000	2.2218 μm	60
HR 1998 ^a	Dec. 19, 1997	14:07	4	960	2.2218 μm	230
Hubble 4	Dec. 20, 1997	5:55	12	3600	2.2291 μm	110
HR 8781 ^a	Dec. 20, 1997	4:15	4	360	2.2291 μm	250
61 Cyg B	Dec. 5, 1998	6:17	2	240	2.2291 μm	190
Hubble 4	Feb. 5, 1999	2:23	4	14400	Optical	60
α Leo ^a	Feb. 5, 1999	6:39	1	30	Optical	300

^aUsed as a telluric standard.

Table 2. Best Fitting Nonmagnetic Model Parameters for
Hubble 4

	T_{eff} (K)	$\log g$	[M/H]	$v \sin i$ (km s ⁻¹)
Fit to Data	4158	3.61	−0.08	14.6
Scatter from Data	8	0.05	0.04	0.57
Uncert. from 61 Cyg B	55	0.50	0.02	1.6
Total Uncertainty	56	0.50	0.04	1.7

Table 3. Ti I gf Values

$\lambda(\text{air})$ (μm)	Initial $\log(gf)$	61 Cyg B Fit $\log(gf)$
2.22112	−1.770	−1.637
2.22328	−1.658	−1.558
2.22740	−1.756	−1.632
2.23106	−2.124	−1.940

Table 4. Magnetic Fits

	S	M1	M2	M3	M4	SpP
$f_{0\text{kG}}$	0.29	0.01(01)	0.14(<01)	0.42
$f_{1\text{kG}}$		0.34(03)	...	0.36(<01)	0.37(<01)	0.00
$f_{2\text{kG}}$		0.02(04)	0.52(<01)	
$f_{3\text{kG}}$	0.71	0.50(04)	...	0.51(<01)	0.51(<01)	0.58
$f_{4\text{kG}}$		0.06(02)	0.34(<01)	
$f_{5\text{kG}}$		0.01(01)	...	0.12(<01)	0.12(<01)	
$f_{6\text{kG}}$		0.05(02)	0.00(<01)	
$f_{7\text{kG}}$		0.01(01)	...	0.01(<01)	...	
χ^2	1.95	1.81	1.82	1.75	1.73	1.73
$\Sigma B_i f_i$ (kG)	2.12	2.56	2.40	2.53	2.51	1.72

Note. — Model S is the single component model. The actual field found in the fit 2.98 kG. Reported filling factors for the multi-component models (M1–M4) are the mean of the 100 Monte Carlo trials for each model. The 1σ uncertainty determined from the trials is given in parenthesis. The χ^2 and $\Sigma B_i f_i$ values are for the specific distributions given above. Model SpP is the spot plus plage model. For the 1 kG component, the actual value use in the fit is the equipartition value of 1.26 kG. The last component at 3 kG is the spot component (1,000 K cooler than the quiet atmosphere), and the actual field value recovered from the fit is 2.97 kG.